

112 3000-
N 35-012
117082
38P

**THE EVALUATION OF A DEFORMABLE DIFFRACTION GRATING
FOR A STIGMATIC EUV SPECTROHELIOMETER**

**Progress Report for NASA Grant NAGW-540
for the period 1 June to 30 November 1987**

**(NASA-CR-182371) THE EVALUATION OF A
DEFORMABLE DIFFRACTION GRATING FOR A
STIGMATIC EUV SPECTROHELIOMETER Progress
Report, 1 Jun. - 30 Nov. 1987 (Stanford
Univ.) 38 P**

N88-14337

**Unclas
0117082**

CSCL 14B G3/35

**J. G. Timothy
Principal Investigator**

**Center for Space Science and Astrophysics
Stanford University
Stanford, California 94305-4055**

During the past six months we have completed the detailed analyses of the initial measurements of the first two toroidal gratings with the correct aspect ratio. The preprint of the paper submitted to Applied Optics is attached to this progress report. In addition, we have continued to refine our concept of the high-resolution spectroheliometer for a Black Brant sounding rocket and a brief report was presented at the e-HRSO workshop. This report is also attached.

The laboratory spectrometer for the detailed tests of the toroidal grating at EUV wavelengths, using the open-structure MAMA detector, has been delivered to the University of Padua, although later than expected. Internal pressures of the order of 2×10^{-7} torr have been achieved. We are now in the process of detailing the mounting system for the detector, including the design of ion traps to prevent the detection of positive ions by the open-structure detector system. The adaptor flange is being fabricated at Stanford. In addition, we are fabricating at Stanford two sets of pinholes for the tests, one set with 20-micron-diameter holes and a second set with 15-micron diameter holes. Each set will have spacings of 250 microns and 500 microns, respectively. We currently hope to start the initial tests in Padua in March or early April. Our data recording and display system is being further upgraded and we will be able to record and display images with formats of 256×1024 pixels or 1024×1024 pixels in real time at Stanford or at Padua.

The deformable substrates for the aspheric gratings required to correct higher-order aberrations have been delivered to ETH Zürich. These will be hand carried to Hyperfine in Boulder, Colorado and the fabrication of the first grating is expected to start in March 1988. The fabrication time will be about 10 months.

Under a separate NASA contract, we are about to start the fabrication of the first MAMA detectors with 14×14 microns² pixels. High-gain MCPs with 8- and 6- micron-diameter channels are also being fabricated. There will be available for tests of the toroidal and aspheric gratings. Advanced versions of these detectors would be used in the flight spectroheliometer.

The Initial Evaluation of
An Imaging Extreme Ultraviolet Spectrometer
Employing a Single Toroidal Diffraction Grating

M.C.E. Huber *

Space Science Department of the
European Space Agency (ESA), ESTEC,
Postbus 299, NL-2200 Noordwijk,
The Netherlands

J. G. Timothy and J. S. Morgan

Center for Space Science and Astrophysics,
ERL 314, Stanford University
Stanford, CA 94305 U.S.A.

G. Lemaître

Observatoire de Marseille
2 place Le Verrier, F-13004, Marseille, France

G. Tondello
Dipartimento di Elettronica ed Informatica, Università di Padova
6/A via Gradenigo, I-35100 Padova, Italy

E. Jannitti and P. Scarin

Istituto Gas Ionizzati, CNR, 6/A via Gradenigo, I-35100
Padova, Italy

Submitted to Applied Optics Received _____

*Currently on leave from Institut für Astronomie, ETH-Zentrum,
CH-8092 Zürich, Switzerland

ABSTRACT

A high-efficiency, extreme ultraviolet (EUV) imaging spectrometer has been constructed and tested. The spectrometer employs a concave toroidal grating illuminated at normal incidence in a Rowland circle mounting and has only one reflecting surface. The toroidal grating has been fabricated by a new technique employing an elastically-deformable sub-master grating which is replicated in a spherical form and then mechanically distorted to produce the desired aspect ratio of the toroidal surface for stigmatic imaging over the selected wavelength range. The fixed toroidal grating used in the spectrometer is then replicated from this surface. Photographic tests and initial photoelectric tests with a two-dimensional, pulse-counting detector system have verified the image quality of the toroidal grating at wavelengths near 600 Å. The results of these initial tests are described in detail and the basic designs of two instruments which could employ the imaging spectrometer for astrophysical investigations in space are briefly described; namely, a high-resolution EUV spectroheliometer for studies of the solar chromosphere, transition region, and corona; and an EUV spectroscopic telescope for studies of non-solar objects.

I. INTRODUCTION

The extreme ultraviolet (EUV) spectral region at wavelengths below $\sim 1200 \text{ \AA}$ is of critical importance for the diagnostics of conditions in high-temperature plasmas since this region contains emission lines and continua characteristic of temperatures in the range from about $10^4 \text{ }^\circ\text{K}$ to greater than $10^6 \text{ }^\circ\text{K}$. This spectral region is thus particularly useful for studies of dynamic phenomena in the outer atmosphere of the sun and other stars. In addition, observations at these wavelengths can provide unique astrophysical data on dynamic phenomena in planetary atmospheres and magnetospheres, on the exchange of matter and energy between stars and the interstellar medium, on the variations of light element abundances in the galaxy and on the dynamics of the hot interstellar gas in galactic haloes.

Because of the lack of window materials and of high-reflectivity optical surfaces at these wavelengths, practical systems for imaging and spectroscopy must employ open-structure detector systems and a minimum of reflecting surfaces. The recent development of high-resolution imaging detector systems which can operate with high efficiency at EUV wavelengths has stimulated the design of optical systems which can provide a stigmatic spectroscopic capability. These imaging spectrometer systems can provide the simultaneous spectral, spatial and temporal resolutions required for many scientific observations that have not been previously possible. In this paper we describe the fabrication and the results of initial tests of a toroidal diffraction grating for use in an imaging EUV spectrometer at wavelengths between 300 and 1200 \AA .

II. SPECTROMETER DESIGN

The design of the spectrometer was stimulated initially by the need for high-time-resolution observations of the solar chromosphere, transition region, and corona with a high spectral resolution ($\lambda/\Delta\lambda \sim 2 \times 10^4$) and a spatial resolution of 1 arc sec or better.¹ The basic configuration of the spectrometer mounting is shown in Figure 1a.

In the conventional Rowland circle mounting, the vertical and horizontal foci from a spherical diffraction grating are not coincident. However, Haber² has pointed out that it is possible to obtain exact stigmatic focusing at two points in the spectrum by selecting the

vertical radius of curvature R_v of a toroidal grating to be smaller than its horizontal radius R_h . As shown in Figure 1a, exact stigmatic focusing can then be obtained at two positions in the spectrum given by:

$$R_v = R_h \cos \alpha \cos \beta_0 \quad (1)$$

The two stigmatic points are located symmetrically to the grating normal at the angles of diffraction $\pm \beta_0$, as shown in Figure 1a. An isometric display of the imaging properties of the two stigmatic points is shown in Figure 1b.

In a practical system where β_0 is small and there is some depth of focus (moderate speed systems with focal ratios $< f/15$), stigmatic focusing can be achieved between and somewhat beyond the two stigmatic points with a simple toroidal surface. Ray tracing studies¹ have shown for a 3600 grooves mm^{-1} grating with a radius of curvature of 2000 mm, blur sizes of significantly less than 40 μm can be obtained over an effective wavelength range of greater than 100 \AA . However, for higher speed systems ($f/10$ or faster), which will be required for astrophysical studies, corrections for higher order aberrations are required.³

A number of high efficiency EUV imaging spectrographic systems can be constructed using this type of diffraction grating. For example, as shown in Figure 2a, the toroidal grating spectrograph can be combined with a normal-incidence Gregorian telescope to produce a high-resolution EUV spectroheliometer for high-spatial-resolution studies of the solar chromosphere, transition region, and corona. Alternatively, as shown in Figure 2b, the toroidal grating spectrograph can be combined with a Wolter type-II grazing-incidence telescope for astrophysical studies at wavelengths below 1200 \AA .

III. GRATING FABRICATION

In order to evaluate the performance characteristics of a toroidal grating at EUV wavelengths, we have fabricated a toroidal replica grating using a unique technique developed by Lemaître.⁴ This technique uses an elastically-deformable grating which is replicated from a spherical master ruling. The ratio of the vertical and horizontal radii of curvature can then be set to any desired value by applying a distorting force to the flexible substrate. The stainless steel flexible substrate (see Figure 3) has a form which elastically deforms into an exact toroidal surface with the application of a single adjustable distorting

force.⁵ The grating, with a ruling frequency of 3600 grooves mm⁻¹, and an active area of 70 x 70 mm² was replicated onto the deformable concave substrate by Hyperfine Inc.,⁶ from a concave spherical master ruling using an intermediate convex replicating surface. A radius-of-curvature of 1000 mm was selected for the initial grating for convenience in laboratory testing. After the substrate had been deformed to the appropriate aspect ratio, a fixed concave toroidal grating was replicated from the deformable substrate, again using an intermediate convex replicating surface. The way in which the forces are applied to the deformable substrate is shown in Figure 4.

The aspect ratio of the toroidal surface was determined in two ways: first, by using a modified, laser-illuminated Martin-Watt-Weinstein version of the Twyman-Green interferometer,^{7, 8, 9} and second, by determining the angle for stigmatic imaging in the zeroth order. The set up of the modified Martin-Watt-Weinstein interferometer with unequal path lengths is shown in Figure 5a. The reference surface was a concave spherical mirror with a radius of curvature of 400 mm. If the grating were spherical, the wavefronts from both the reference and grating surfaces would be identical (spherical), producing a uniform illumination in the recombined beam. When the grating figure is toroidal, a saddle surface is superimposed on the sphere and, accordingly, fringes exhibit a saddle path in the recombined beam over the projection of the test surface. The maximum deviation of the grating surface from a sphere occurs in the directions where there are the greatest number of fringes from the center to the edge. In these directions the difference in height between the toroid and the reference sphere is equal to $\frac{N\lambda}{2}$, where N is the number of fringes from the center to the edge and λ is the wavelength of the laser (6325 Å). The total deviation Δ across the complete toroidal surface is then given by $\Delta = \frac{2N\lambda}{2}$, where $\Delta = h_v - h_h = \frac{a^2}{2} \left(\frac{1}{R_v} - \frac{1}{R_h} \right) \sim \frac{a^2}{2R^2} (R_h - R_v)$, with a being the half width of the grating and R being the mean radius of curvature of the grating.

The aspect ratio R_v/R_h is then determined from

$$\frac{R_v}{R_h} = \frac{R - \left(\frac{R_h - R_v}{2} \right)}{R + \left(\frac{R_h - R_v}{2} \right)} = \frac{1 - \frac{R}{a} \Delta}{1 + \frac{R}{a} \Delta} = \frac{a - R\Delta}{a + R\Delta} \quad (2)$$

The second measurement technique is shown in the schematic in Figure 5b. Since from equation 1,

$$\frac{R_v}{R_h} = \cos \alpha \cos \beta_0 \quad (3)$$

it follows that for the symmetrical case of stigmatic imaging in zeroth order, where $\alpha = \beta_0 = \gamma$,

$$\frac{R_v}{R_h} = \cos^2 \gamma \quad (4)$$

The "angle of reflection" γ is determined by measuring the position of best focus for the 1:1 image of a pinhole .

The desired characteristics of the grating for imaging at wavelengths near 600 Å are given in Table 1. Three toroidal replica gratings have been fabricated to date. The symmetry of the toroidal surface was excellent in all cases as shown by the uniformity of the classic "saddle" fringe pattern (see Figure 6). Since toroidal gratings have been identified for possible use on the ESA/ NASA Solar and Heliospheric Observatory (SOHO) mission and the *Lyman* EUV Spectroscopic Explorer mission, the grating was subjected to a thermal vacuum test over the temperature range from - 20° C to + 40° C. No change in the aspect ratio was observed, as can be seen from a comparison of Figures 6a and 6b. The estimated uncertainty of these measurements was less than ± 1 fringe.

The results from both measurement techniques agreed to within the experimental error. The first grating received from Hyperfine Inc. had too low an aspect ratio of 0.9892 which would produce stigmatic images on the normal at wavelengths near the 400 Å when used at an angle of incidence of 8°43. However, the second and third replicas were essentially identical with aspect ratios of 0.9809 close to the desired value of 0.9782. The reasons for the lower than expected aspect ratios are currently being investigated with Hyperfine Inc. At an angle of incidence of 11°.2 the wavelength on the grating normal is 540 Å and an acceptable imaging performance over the wavelength range from 520 to 630 Å was obtained by slightly changing the angle-of-incidence.

IV. TEST RESULTS

Initial tests of the imaging properties of the toroidal grating at EUV wavelengths were carried out using a specially designed laboratory spectrometer. First, spectral images from a line of ten pinholes arranged along the entrance slit and illuminated by a low-voltage, low-pressure spark-discharge source were recorded on photographic film. The pinholes were drilled in aluminum foil with a laser and had diameters ranging from 10 to 33 μm . The distance between adjacent pinholes was 500 μm . The EUV spectral images of the pinholes recorded on Schumann emulsion located along the Rowland circle are shown in Figure 7a. The stigmatic focus points are marked by arrows. Densitometer measurements of these photographic images show that the spatial variation of the blur dimensions agrees with that predicted from the ray trace analyses¹ (see Figure 7b).

Because of the difficulties associated with the analysis of the non-linear intensity data in the photographic images, data were also recorded at the wavelength of the He I resonance line at 584 \AA with an imaging photoelectric detector system having a linear response. For these tests a dc hollow-cathode light source was employed. The photographic plate was replaced with a tetraphenyl-butadiene phosphor applied to a glass plate mounted on the Rowland circle. This phosphor down-converts EUV photons into visible-light photons with a peak emission near 4300 \AA .¹⁰ The visible-light images were viewed through a window in the vacuum tank and re-imaged and magnified by approximately a factor of three onto the photocathode of a visible-light Multi-Anode Microchannel Array (MAMA) detector tube¹¹ using the optical system shown in the schematics in Figure 8.

As shown in Figure 9a, the imaging visible-light MAMA detector tube employs a bi-alkali semi-transparent photocathode in proximity focus with a high-gain curved-channel microchannel plate (MCP) and has a readout anode array of precision electrodes to produce a format of 256 x 1024 pixels with pixel dimensions of 25 x 25 μm^2 . The complete detector head assembly is shown in Figure 9b. Details of the readout array have been described recently by Timothy.¹² The detector operates as a pulse-counting system with zero read-out noise. The dark count from the bi-alkali photocathode at room temperature was of the order of 5 counts s^{-1} for the whole array. For these measurements a set of pinholes with separations of 250 μm was employed. The magnifying optics gave an effective spatial resolution for each detector pixel of about 8 μm on the Rowland circle of

the spectrograph. The two-dimensional digital images obtained from the MAMA detector in the laboratory were recorded on a portable data handling and display system.

A one-dimensional cut through the line of ten pinholes along the entrance slit at the wavelength of 584 Å resonance line is shown in Figure 10. Because of the low transfer efficiency of the phosphor and the lens system, it was only possible in these initial tests to record images at the wavelength of the strong He I resonance line. In order to determine the modulation transfer function of the phosphor and the lens system after the EUV images had been recorded, the pinholes were attached to the phosphor and back-illuminated by an incandescent lamp. The two image profiles are shown in Figure 11a. Convolution of the two sets of images show that the maximum spatial blur dimensions introduced to the toroidal grating are below 25 µm as predicted from the ray trace analyses. The convolved image of the pinhole image compared with the grating image is shown in Figure 11. On a root-sum-square basis the spatial aberrations introduced by the grating at this wavelength are calculated to be about 16 µm (FWHM).

Two-dimensional images recorded with the MAMA detector showing the self-reversal of the He I 584 Å resonance line for two different gas pressures in the light source are shown side-by-side in Figure 12. The difference in the line widths for one of the pinhole images when the hollow cathode lamp is run at low and high gas pressures is shown in Figure 13. The measured difference in the line widths is 0.14 Å (FWHM). As the depth and the width of the self-reversal is not known the spectral resolution could not be determined in these tests. A rough estimate of the saturated self-reversed part of the profile leads to a width of 19 mÅ, corresponding to about 7 µm on the Rowland circle. Zero intensity in the self-reversed part of the line profile would not be expected, given the calculated aberrations and the measured modulation-transfer of the phosphor-lens system.

V. SUMMARY

Initial tests have shown that a single toroidal diffraction grating produced by a simple procedure utilizing an elastically-deformable substrate has excellent imaging characteristics at EUV wavelengths. More detailed tests of the imaging properties of the toroidal grating over a wider range of wavelengths will be undertaken shortly with an open-structure version of the two-dimensional (256 x 1024)-pixel MAMA detector system, using a laboratory spectrograph which is now under construction at the University of Padua. Studies have also been initiated to define ways of providing corrections for higher order

aberrations in fast systems ($f/10$ or lower), using an elastically deformable substrate with a more complex configuration.

We wish to thank Mr. B. Bach of Hyperfine, Inc. for his efforts with the ruling of the master grating and with the fabrication of the toroidal replica gratings. We also thank R. Haw at Stanford University for assistance with the reduction of the digital data and M. E. Puiatti at the University of Padua for assistance with the reduction of the photographic data. This work was supported in part by the Ministero Pubblica Istruzione, in part by the Schweizerischer Nationalfonds and in part by NASA Grants NAGW-540, NAGW-551 and NASA Contract NASW-4093.

Table 1. Desired characteristics of the test toroidal diffraction grating.

Wavelengths and angles of rays:

Stigmatic wavelength range	520 - 630 Å (first order)
Angle of incidence α	11.947°
Wavelength on grating normal ($\beta = 0^\circ$)	575 Å
Wavelength at stigmatic points ($\beta_0 = \pm 0.825^\circ$)	535 Å, 615 Å

Grating surface:

Horizontal radius of curvature R_h	1011.1 mm
Vertical radius of curvature R_v	989.1 mm
Aspect ratio R_v/R_h	0.9782
Ruling frequency	3600 grooves mm ⁻¹
Ruled area	70 x 70 mm ²

REFERENCES

1. Huber, M.C.E. and Tondello, G., Applied Optics **18**, p. 3948, 1979.
2. Haber, H. J. Opt. Soc. Amer. **40**, p. 153, 1950.
3. Cash, W.C. Jr., Applied Optics **23**, p. 4518, 1984.
4. Leimaître, G., in Optical Telescopes of the Future, ESO Conference, Proc. eds. F. Pacini, W. Richter and R. N. Wilson, p. 321, (1978).
5. Huber, M.C.E., Jannitti, E., Lemaitre, G., and Tondello, G., Applied Optics **20**, p. 2139, 1981.
6. Hyperfine Inc., 4946 North 63rd Street, Boulder, Co. 80301, (303) 530-0709.
7. Born, M., and Wolff, E., Principles of Optics, Pergamon Press, p. 303, (1980).
8. Françon, M., Optical Interferometry, Academic Press, New York and London, p. 202, 1966.
9. Johansson, S. and Litzén, U., Physica Scripta **10**, p. 121 1974.
10. Burton, W. M., and Powell, B. A., Applied Optics **12**, p. 87, 1973.
11. Timothy, J. G., Optical Engineering **24**, p. 1066, 1985.
- 12.. Timothy, J. G., SPIE X-ray Imaging II **691**, p 1986.

LIST OF FIGURES

1. a. Schematic of the imaging EUV spectrometer employing a single toroidal grating. Exact stigmatic focusing is obtained at angles of diffraction $\pm \beta_0$, which are defined by equation 1. Given a sufficiently small value of β_0 and some depth of focus, effective stigmatic focusing can be achieved between and somewhat beyond the two stigmatic points.

 b. Isometric display of the imaging properties at the two stigmatic points $\pm \beta_0$
2. Schematics of telescope and imaging spectrometer systems.
 (a) High-resolution EUV spectroheliometer using a Gregorian telescope.
 (b) Grazing-incidence telescope and normal-incidence spectrograph combination for astrophysical studies at wavelengths below 1200 Å.
3. (a) 3600 grooves mm⁻¹ grating replicated on an elastically-deformable substrate.
 (b) Close-up showing the deforming actuator (a differential micrometer).
4. Form of the elastically deformable substrate. Forces are applied at the indicated points.
5. (a) Schematic of the modified Martin-Watt-Weinstein interferometer for the determination of the aspect ratio of the toroidal grating surface.
 (b) Schematic showing the zeroth-order technique for measurement of the aspect ratio of the toroidal grating surface.
6. Saddle fringe pattern produced by toroidal grating #3.
 (a) Before thermal vacuum test.
 (b) After thermal vacuum test.
7. (a) Spectral images of ten pinholes arranged along the spectrometer entrance slit illuminated by a low-voltage, low-pressure spark source. The arrows indicate the stigmatic wavelengths.

- (b) Spatial blur dimensions (with estimated uncertainties) as determined from the photographic spectra, shown in comparison with the ray-tracing results.
8.
 - (a) Schematic of the optical system for the initial photoelectric tests of the toroidal grating.
 - (b) Detail of the re-imaging system and detector assembly.
 9. (256 x 1024)-pixel MAMA detector system.
 - (a) Schematic of detector tube.
 - (b) Detector head assembly.
 10. One-dimensional image at the wavelength of the He I resonance line at 584 Å of ten pinholes located along the spectrometer entrance slit. The different pinhole diameters (ranging from 10 to 33 μm) results in different peak intensities.
 11.
 - (a) Comparison of the pinhole and phosphor image profile with the image from the complete optical system including the diffraction grating. Solid line, pinhole and phosphor profile, dashed line profile recorded with the toroidal grating.
 - (b) Comparison of convolved pinhole image with the image from the toroidal grating.
 12. Spectral images of the ten pinholes showing the self-reversal of the He I 584 Å resonance line with different gas pressures in the light source. Left, low gas pressure, right, high gas pressure. Good imaging is achieved although the line of pinholes is skew with respect to the normal to the plane of dispersion.
 13. Spectral images from one pinhole showing the width and the depth of the self-reversal of the He I 584 Å resonance line.
 - (a) Low gas pressure.
 - (b) High gas pressure.

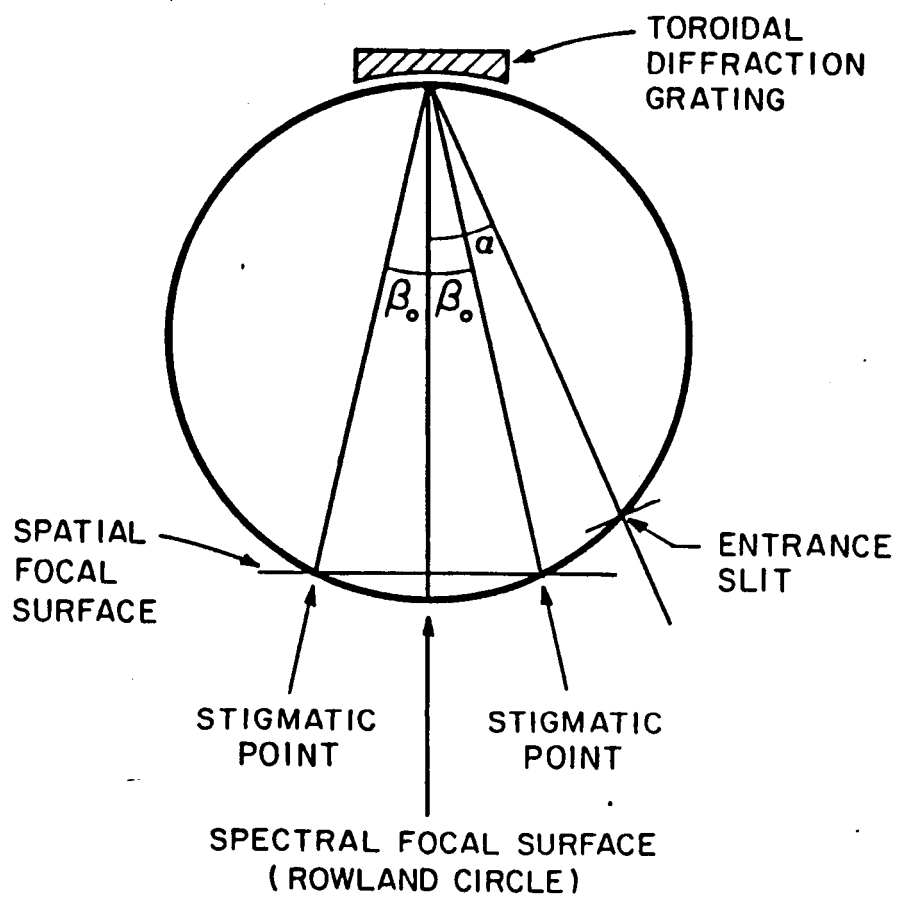


Figure 1a

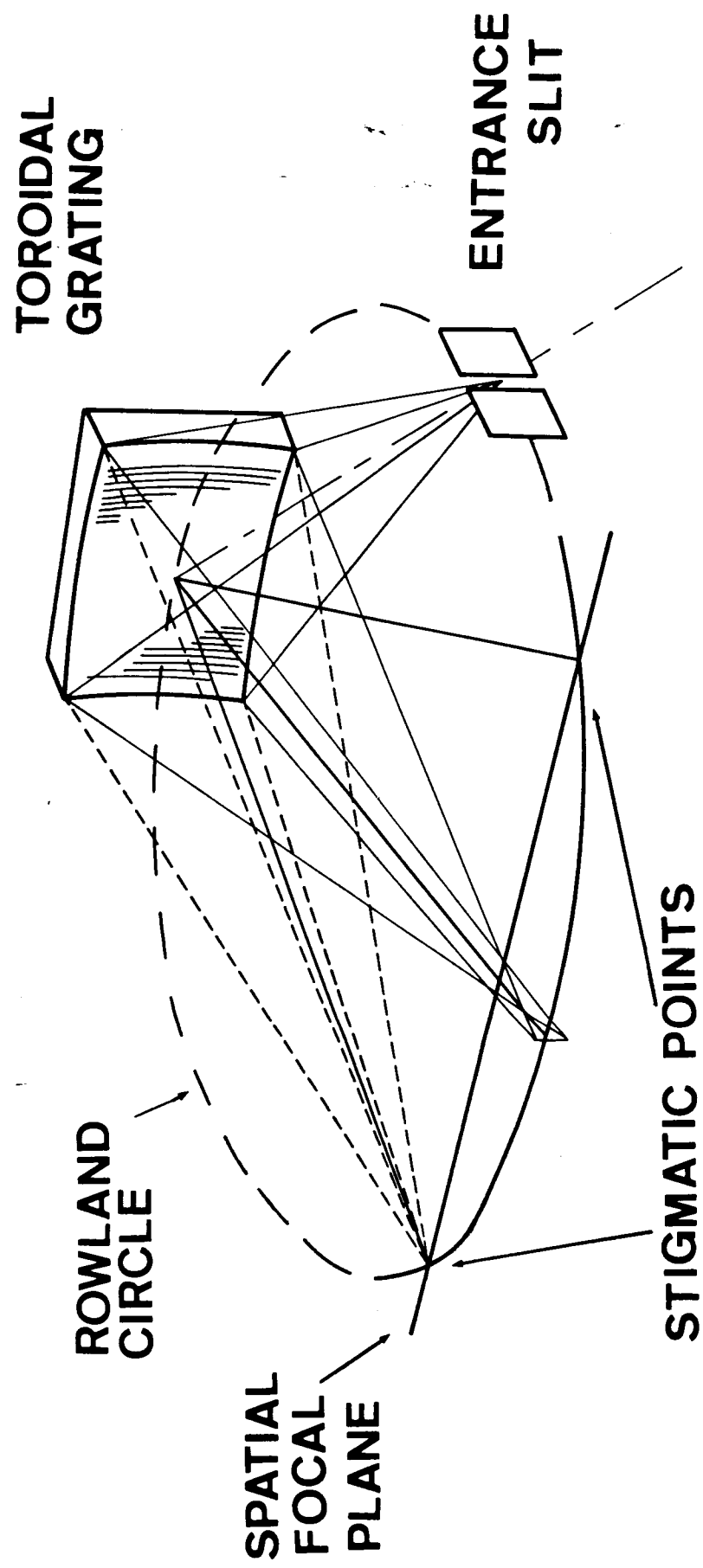


Figure 1 b

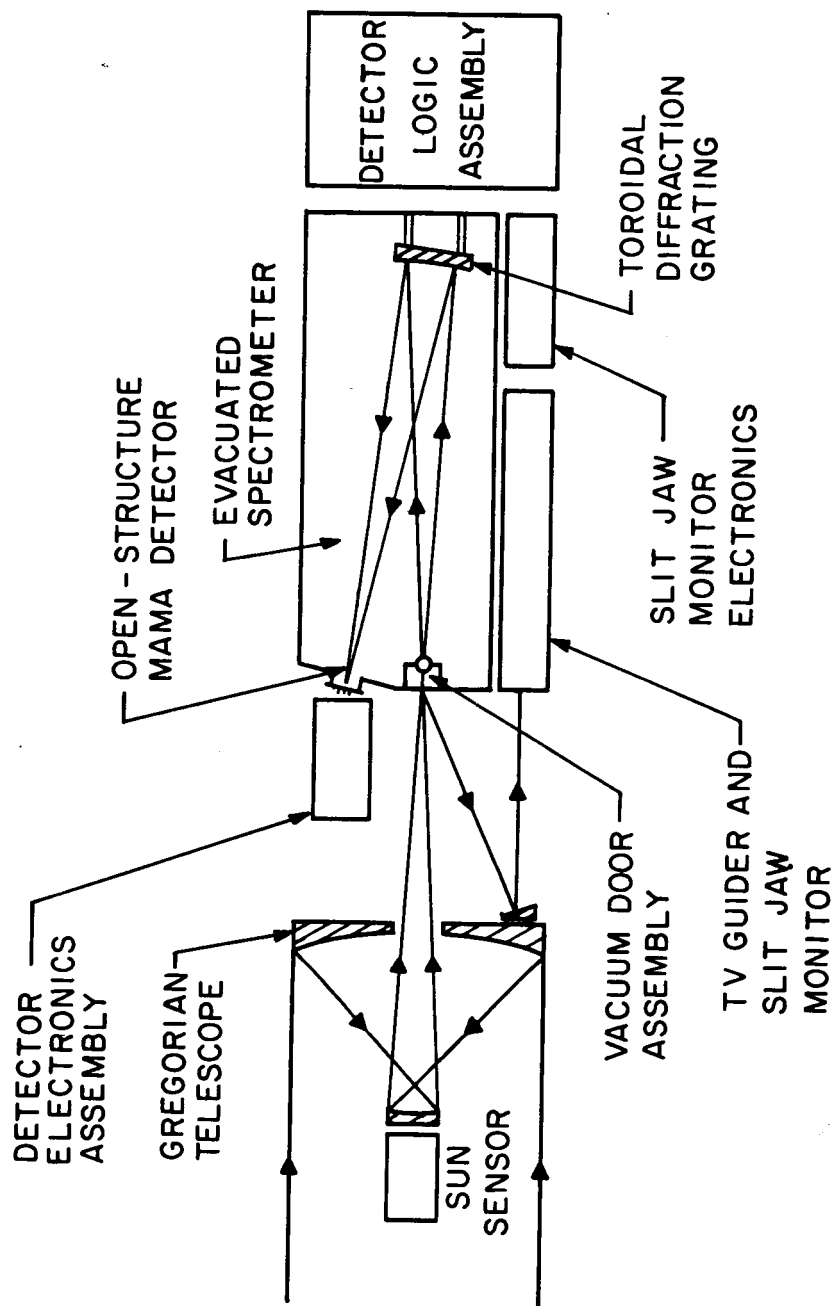


Figure 2 a

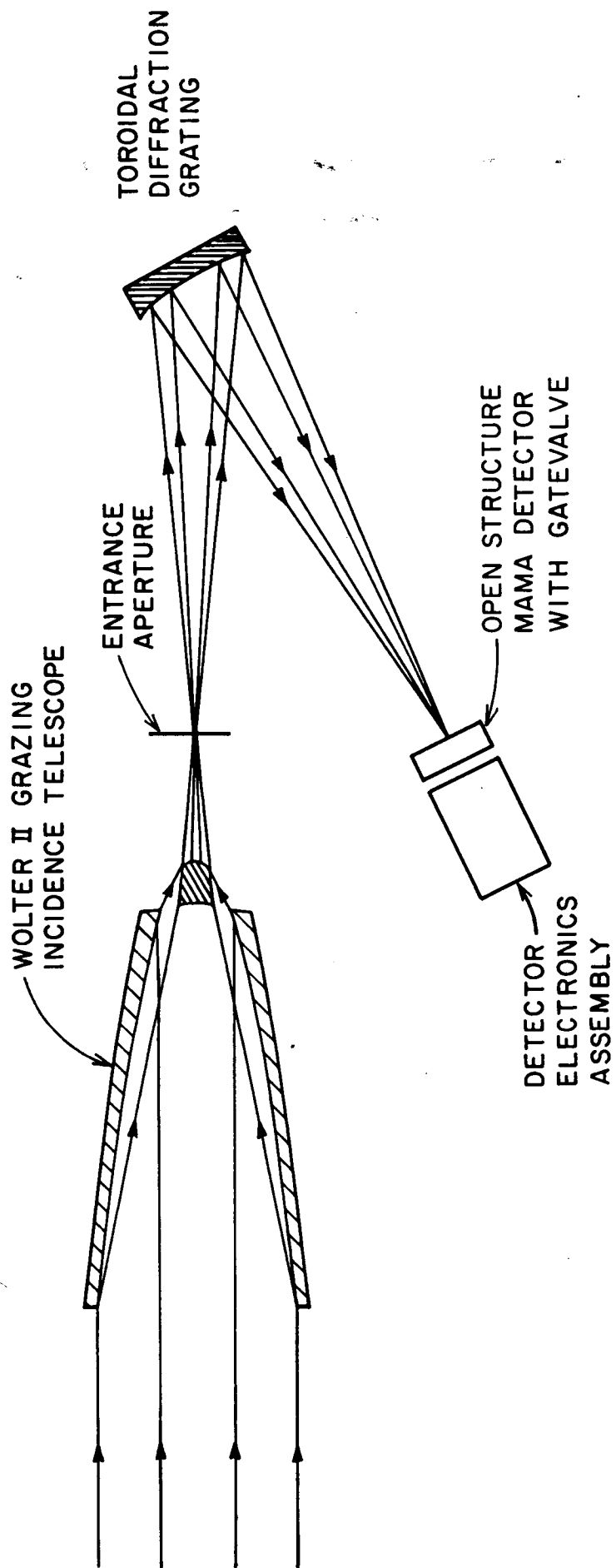


Figure 2 b

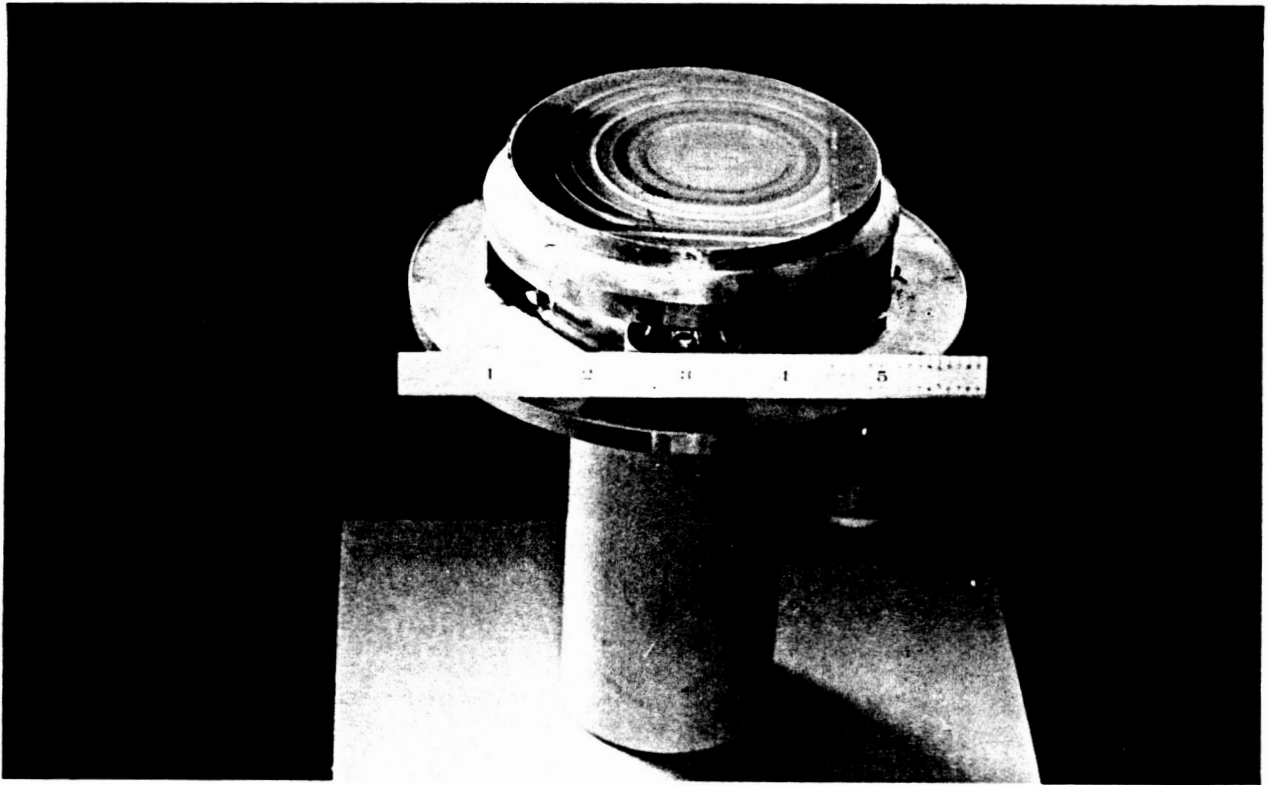


Figure 3 a

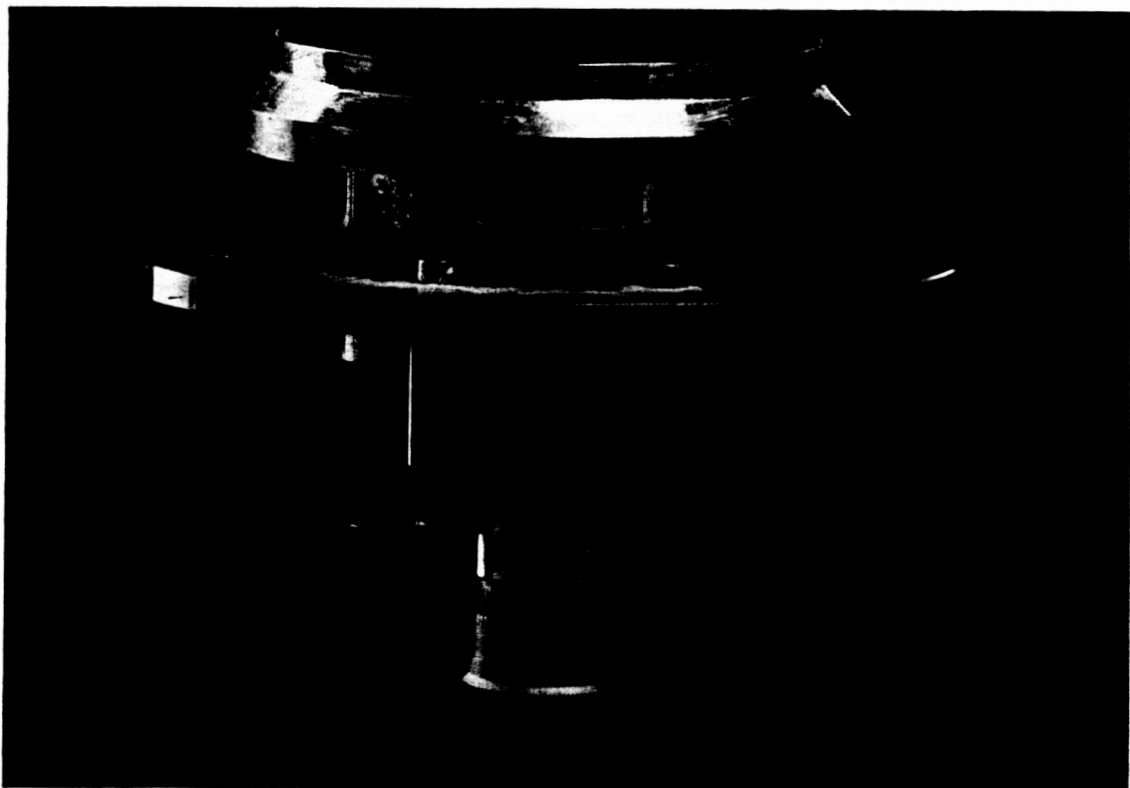
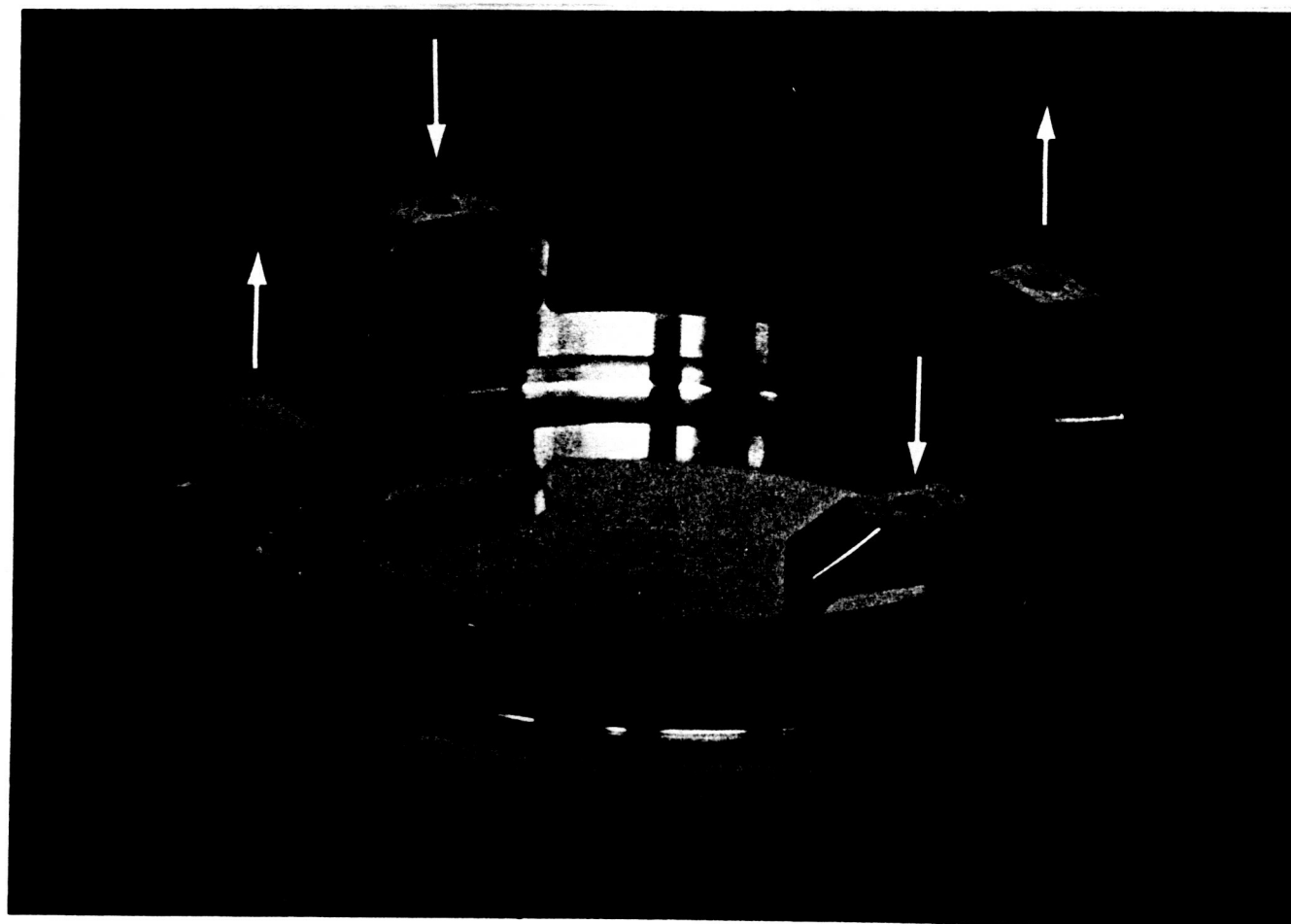


Figure 3 b

ORIGINAL PAGE IS
OF POOR QUALITY



ORIGINAL PAGE IS
OF POOR QUALITY

Figure 4

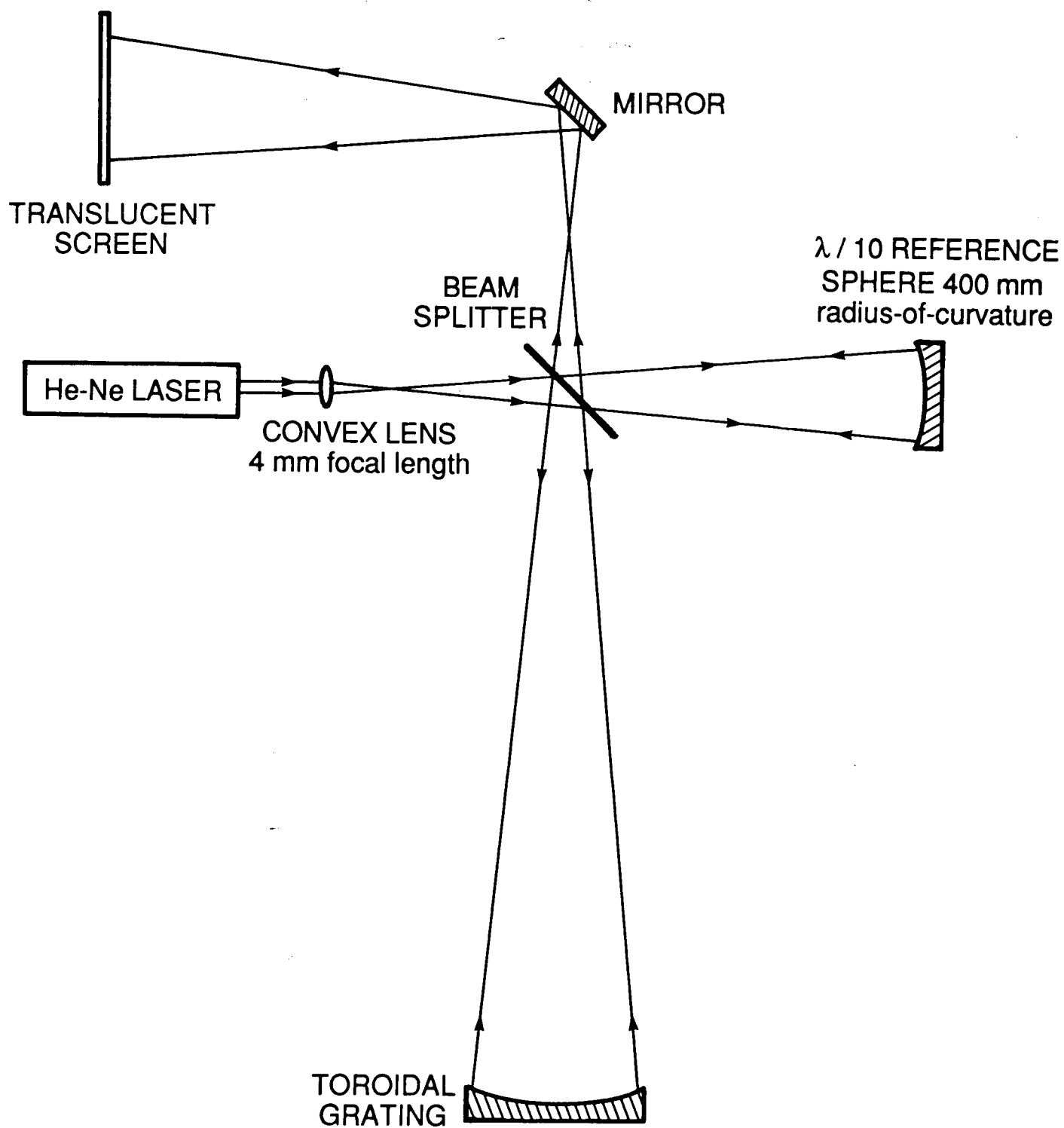


Figure 5a

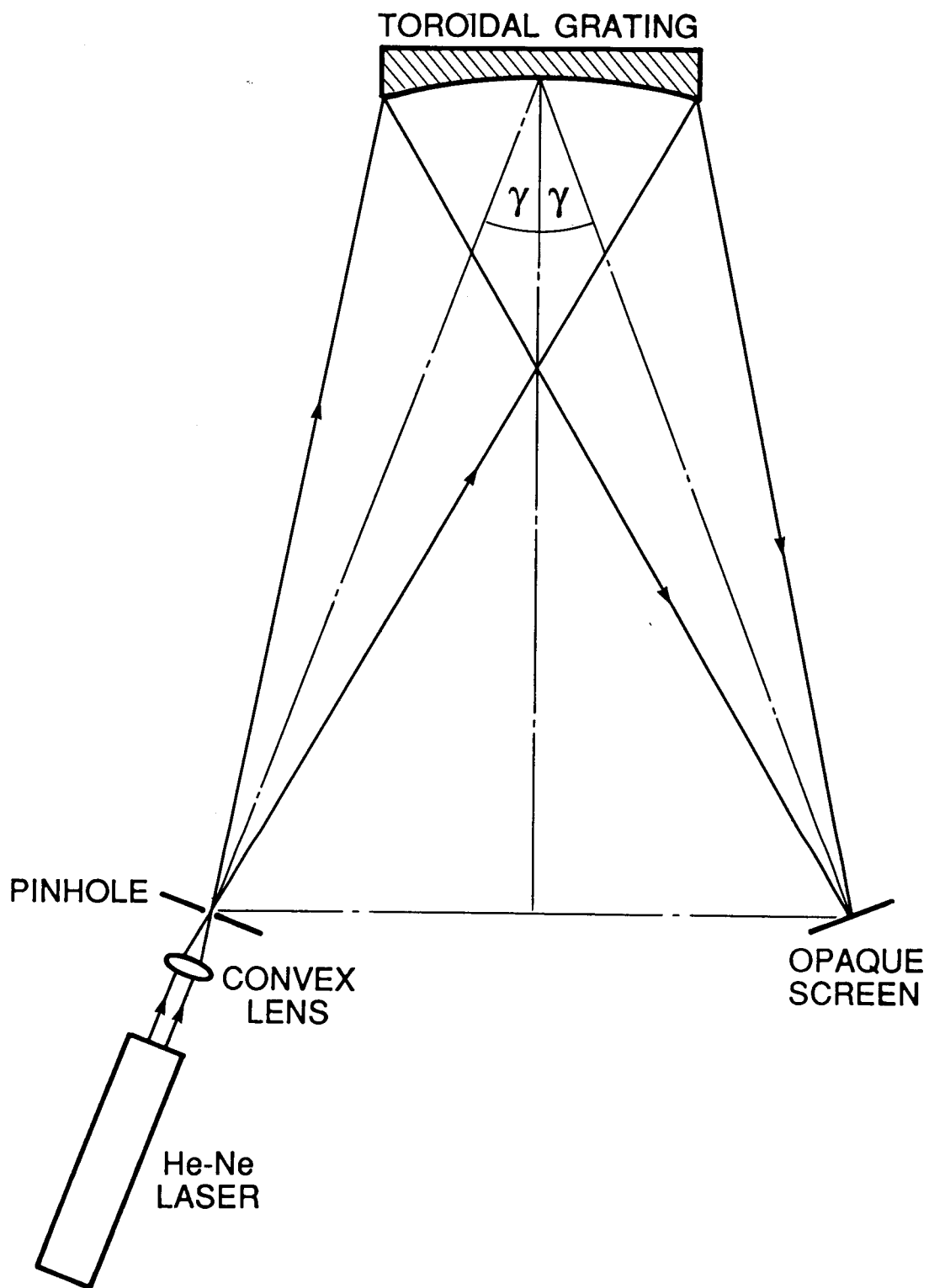


Figure 5b

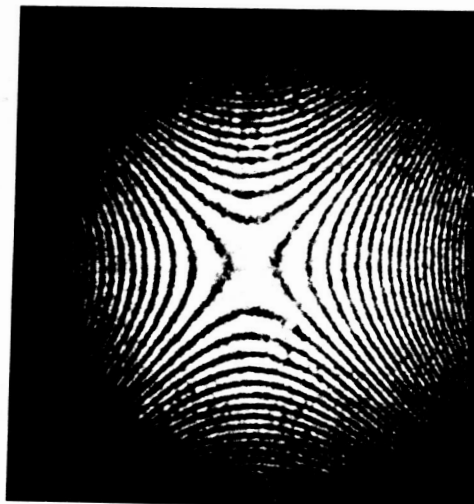


Figure 6 a

ORIGINAL PAGE IS
OF POOR QUALITY

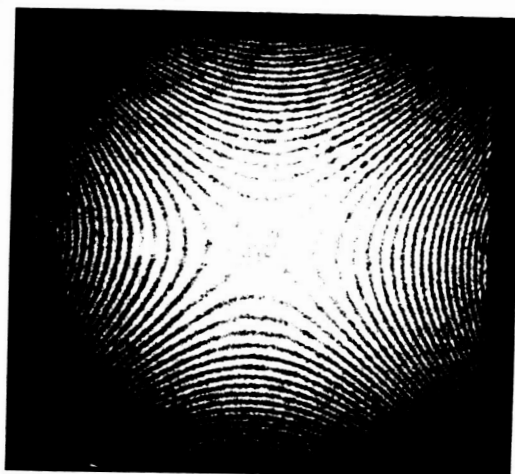
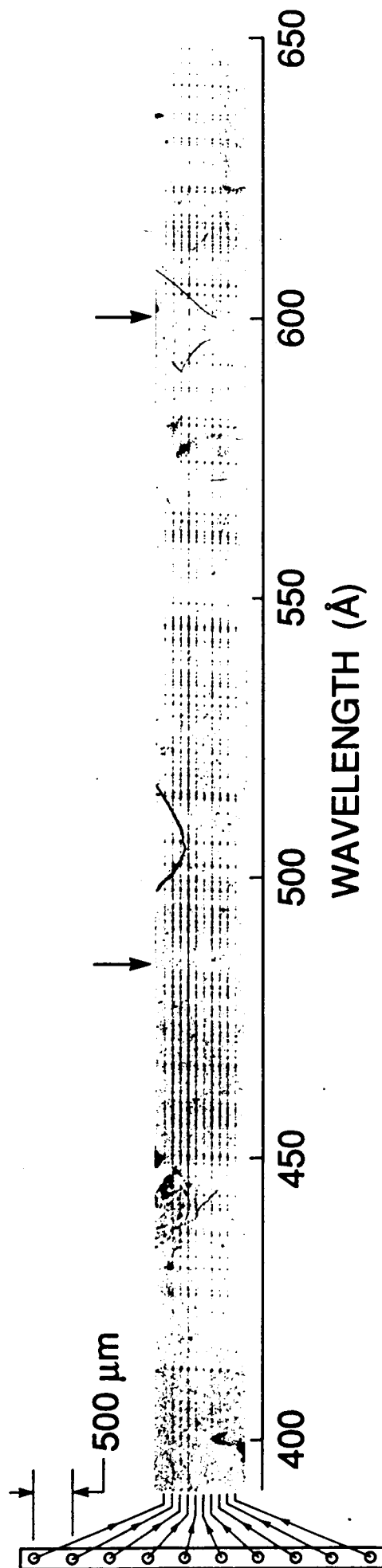


Figure 6 b



ORIGINAL PAGE IS
OF POOR QUALITY

Figure 7 a

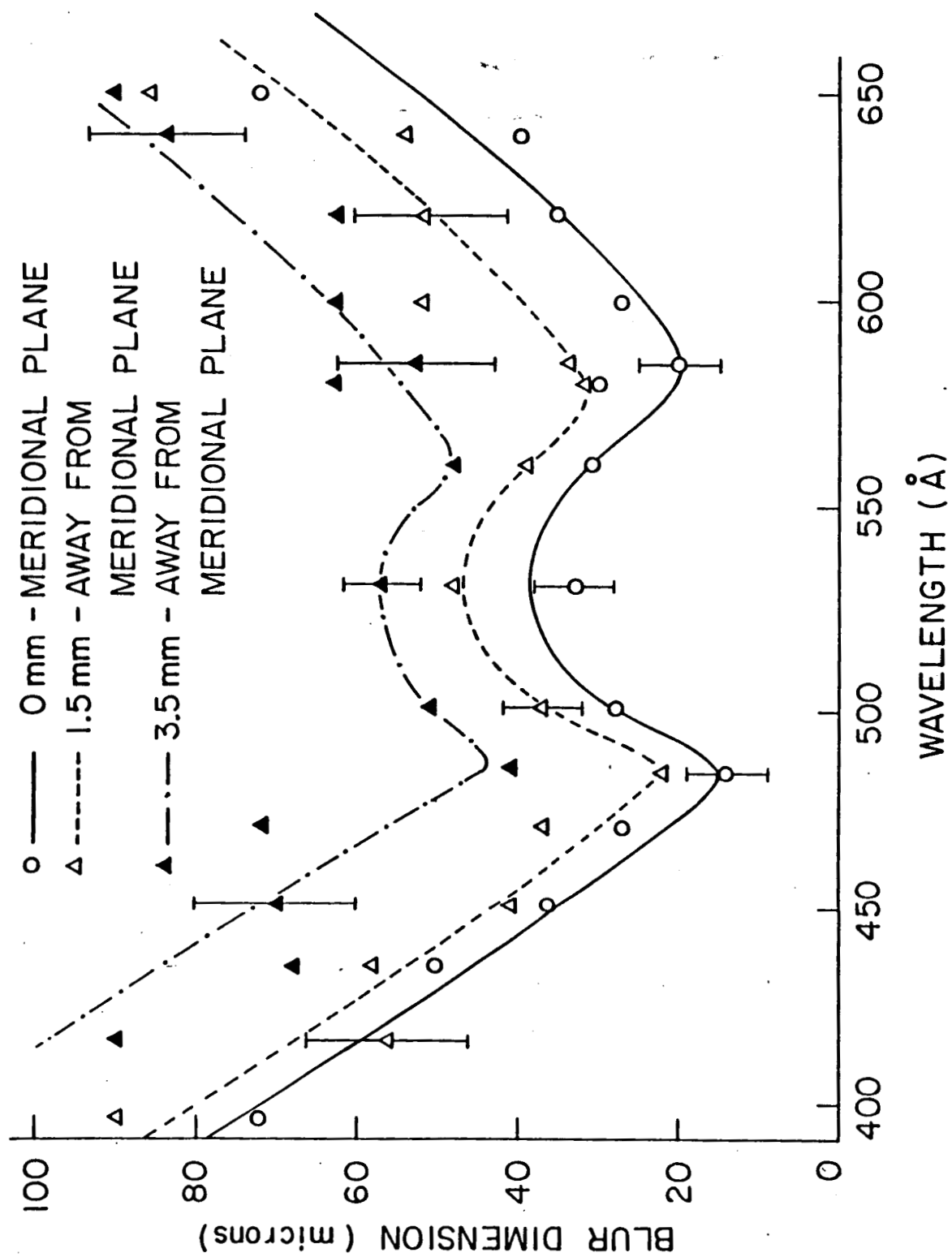


Figure 7b

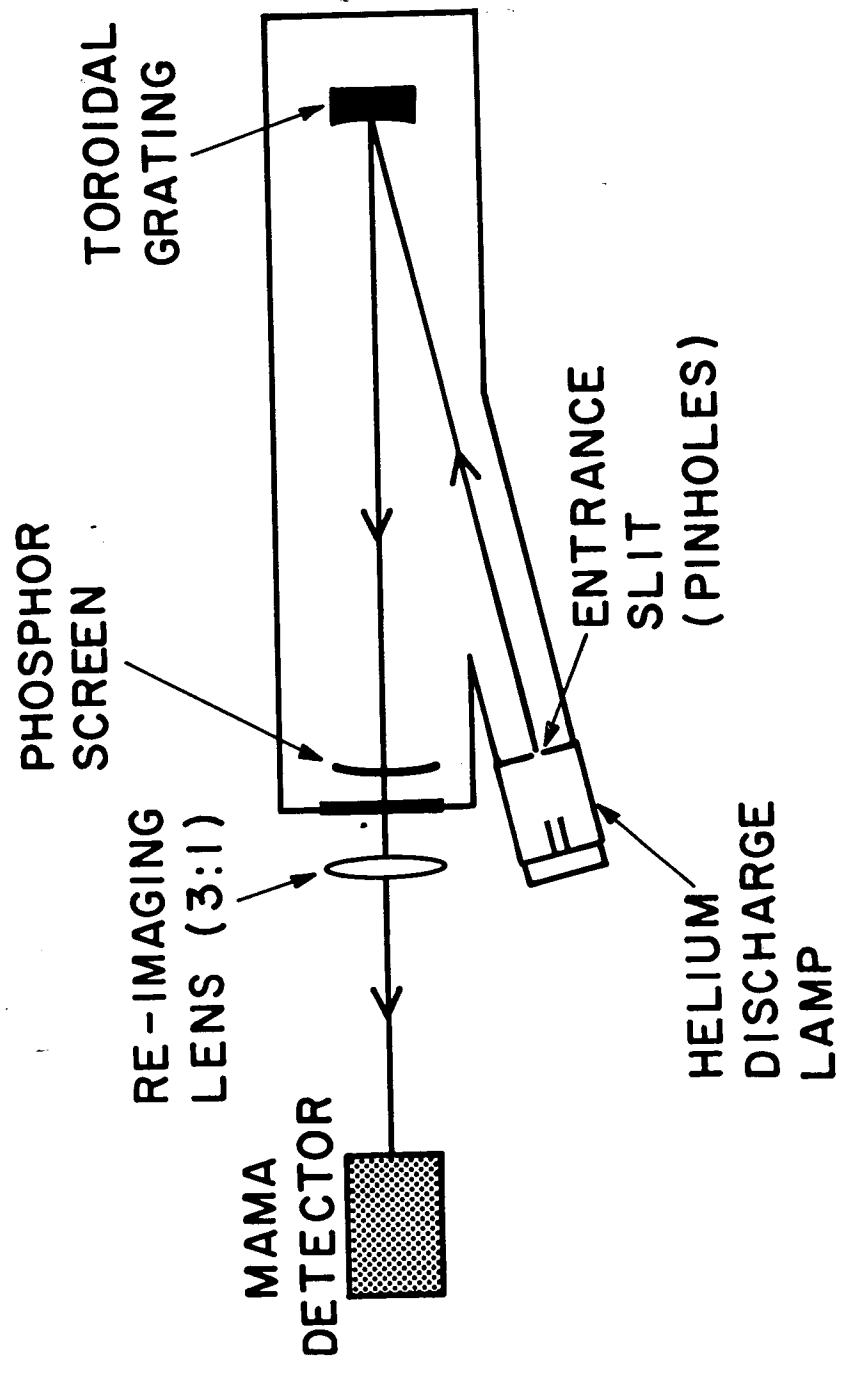


Figure 8 a

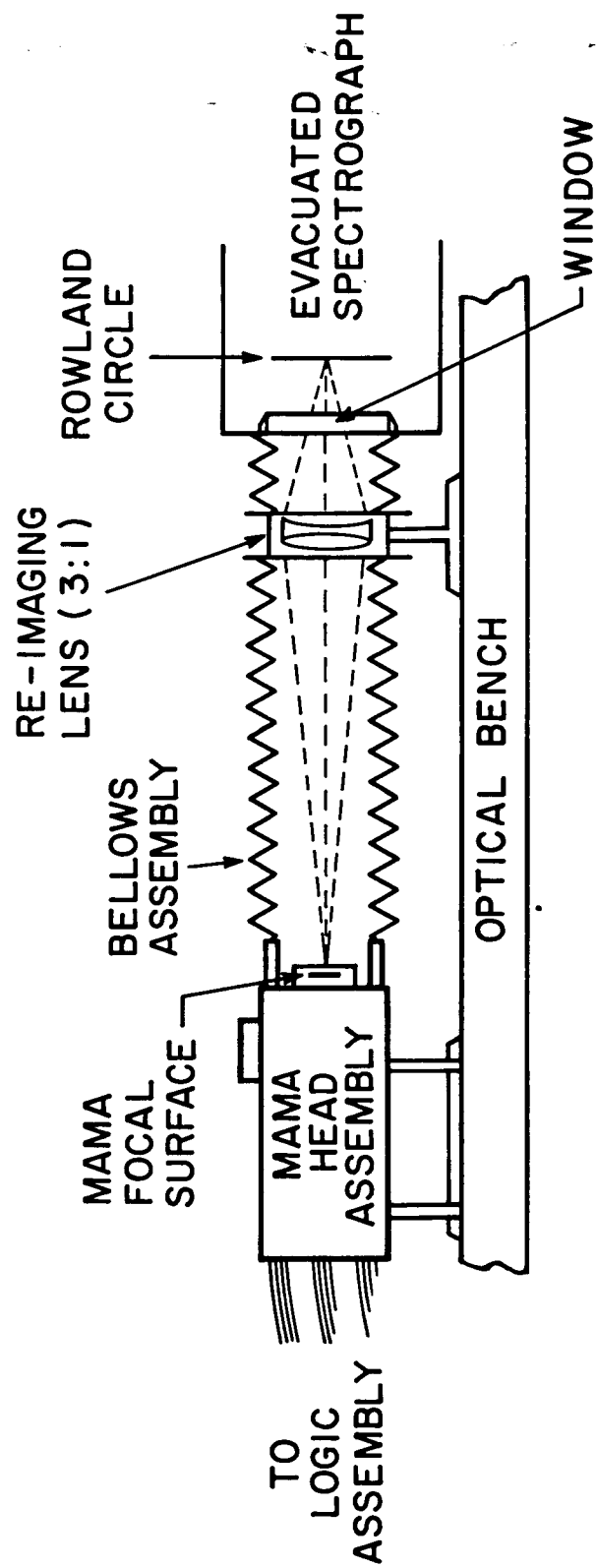


Figure 8b

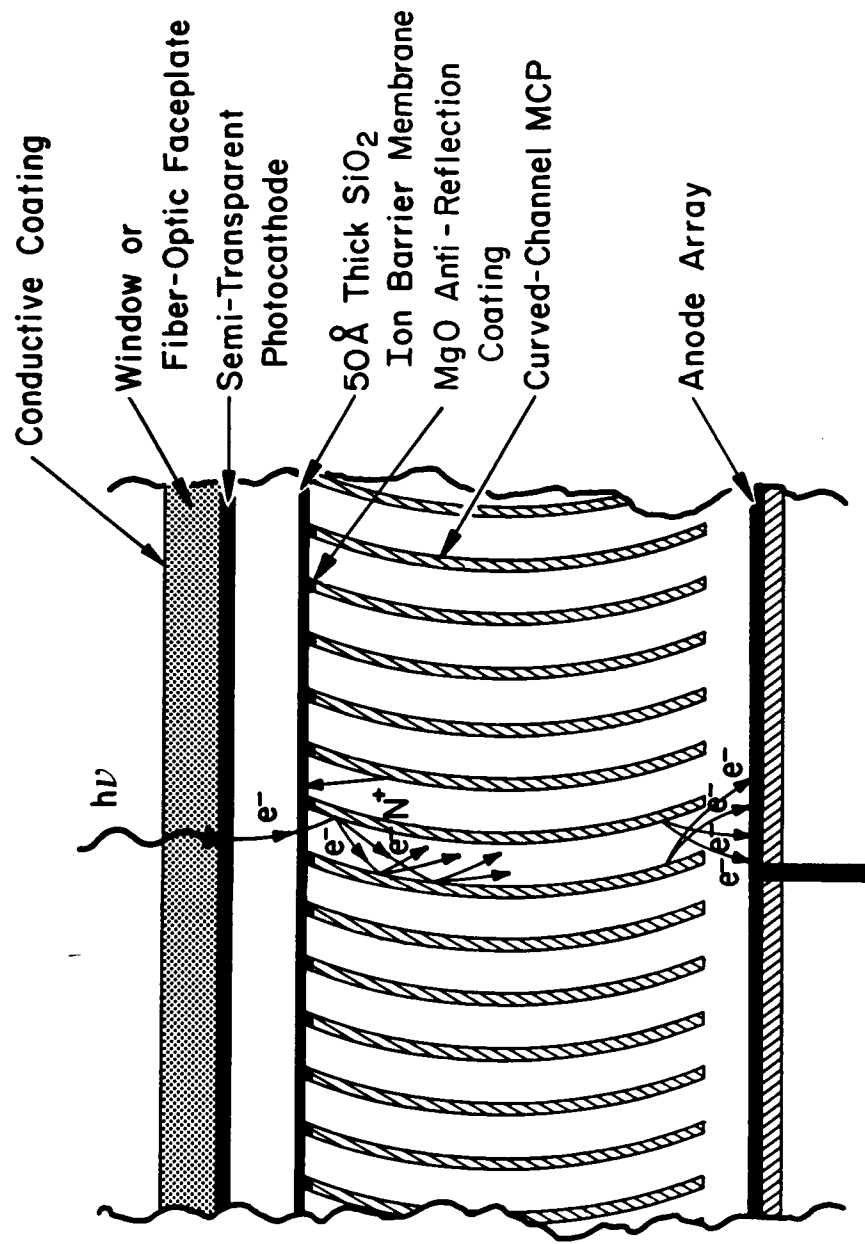
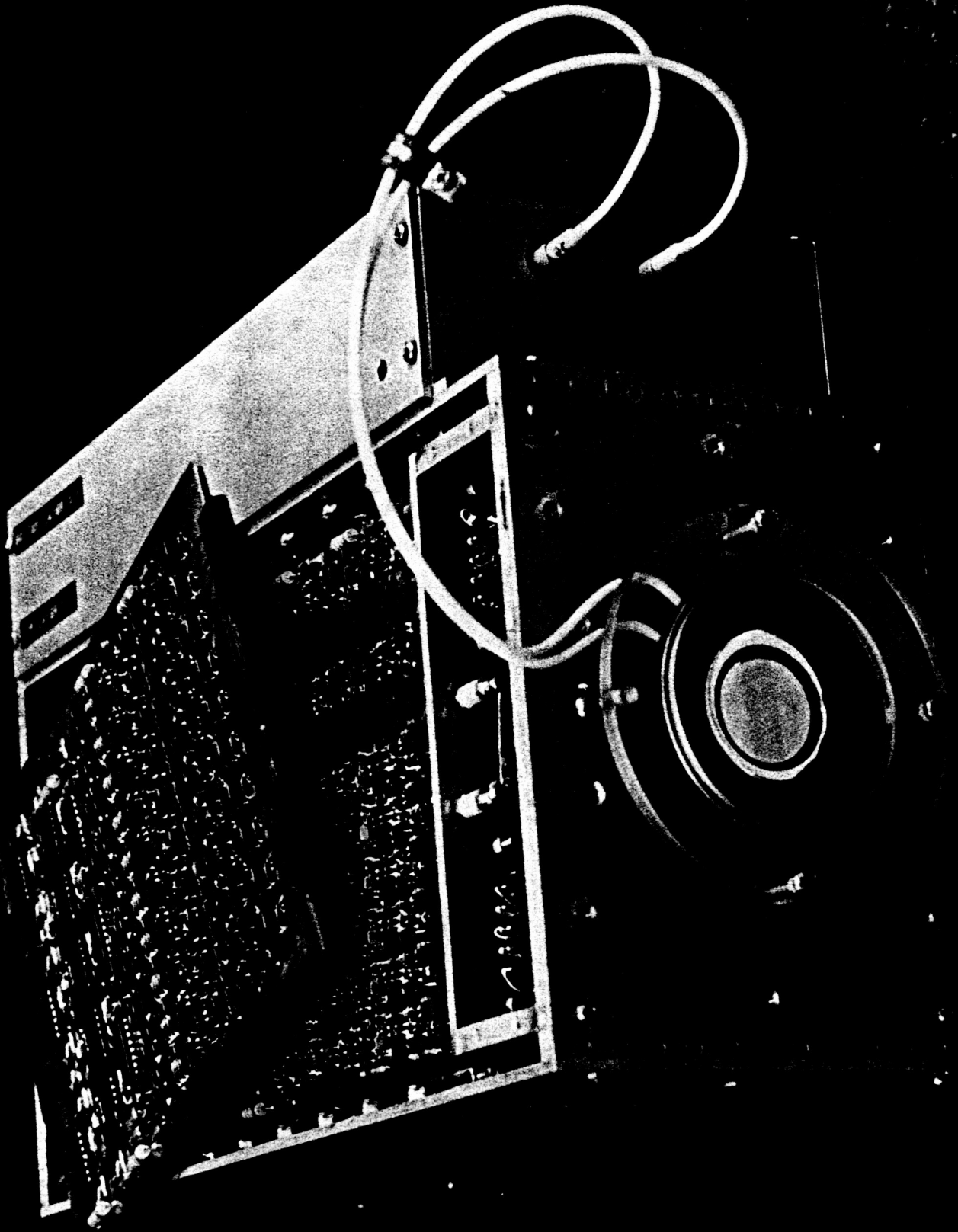


Figure 9a

Figure 9 b



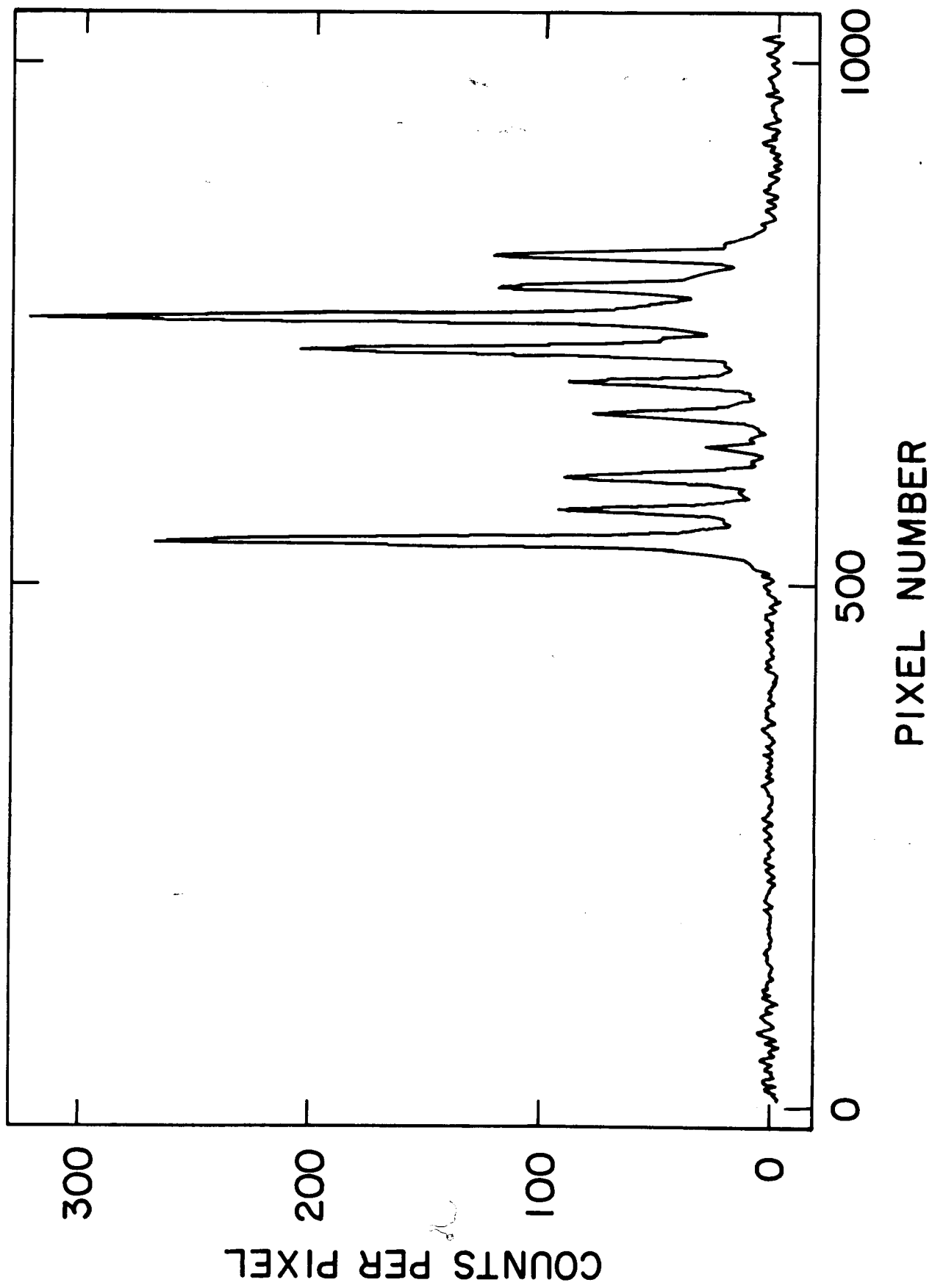


Figure 10

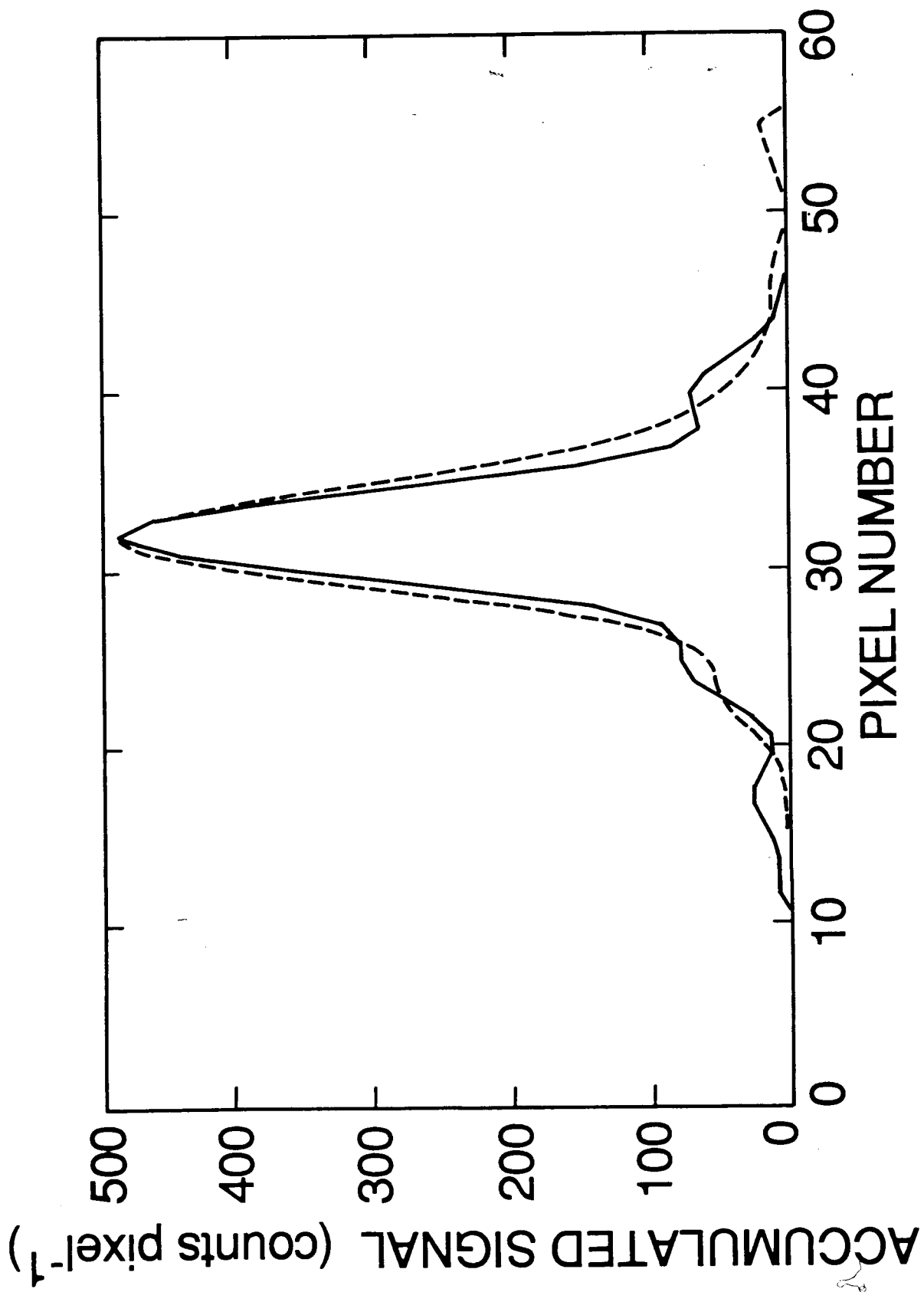


Figure 11 a

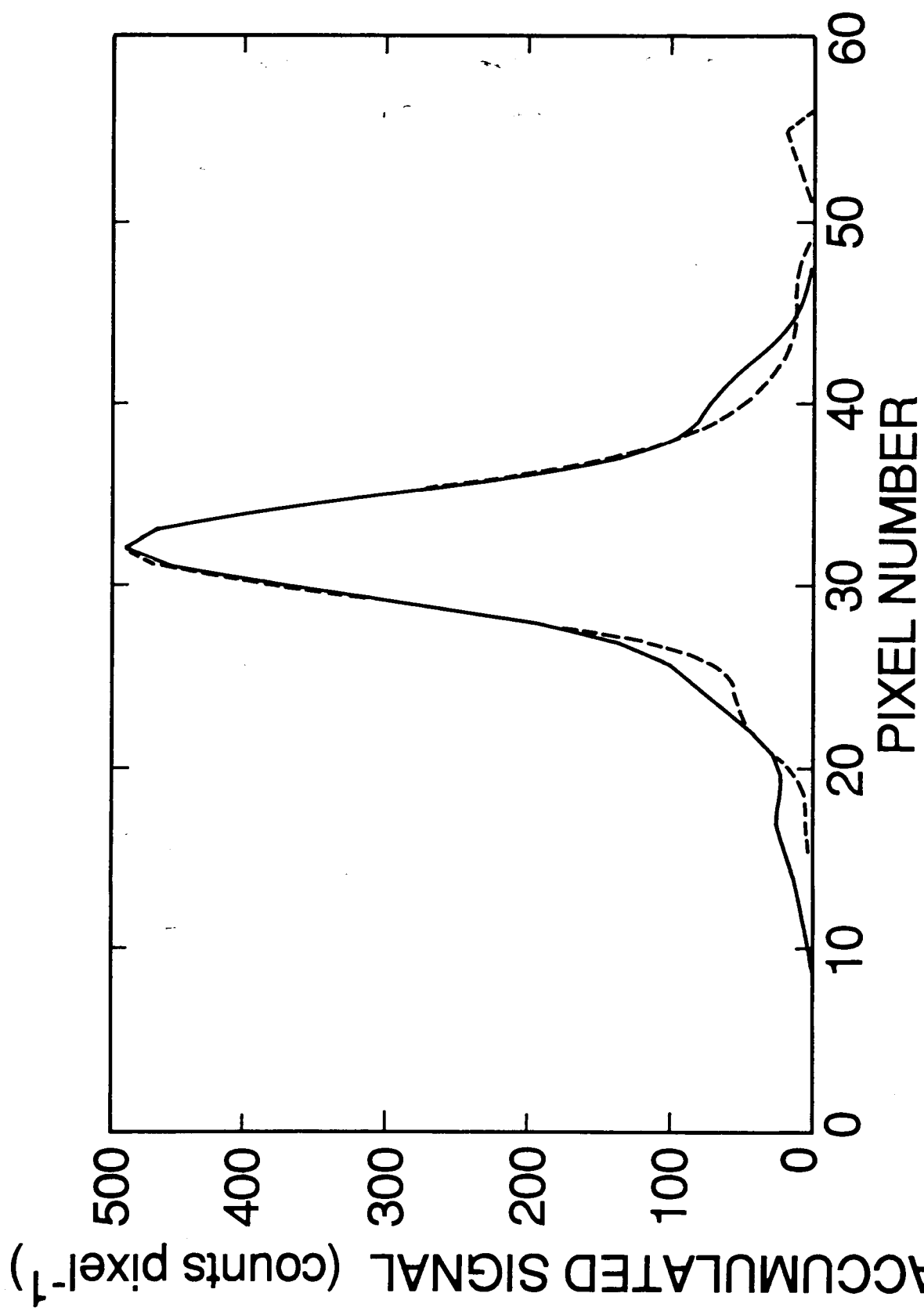


Figure 11 b

ORIGINAL PAGE IS
OF POOR QUALITY

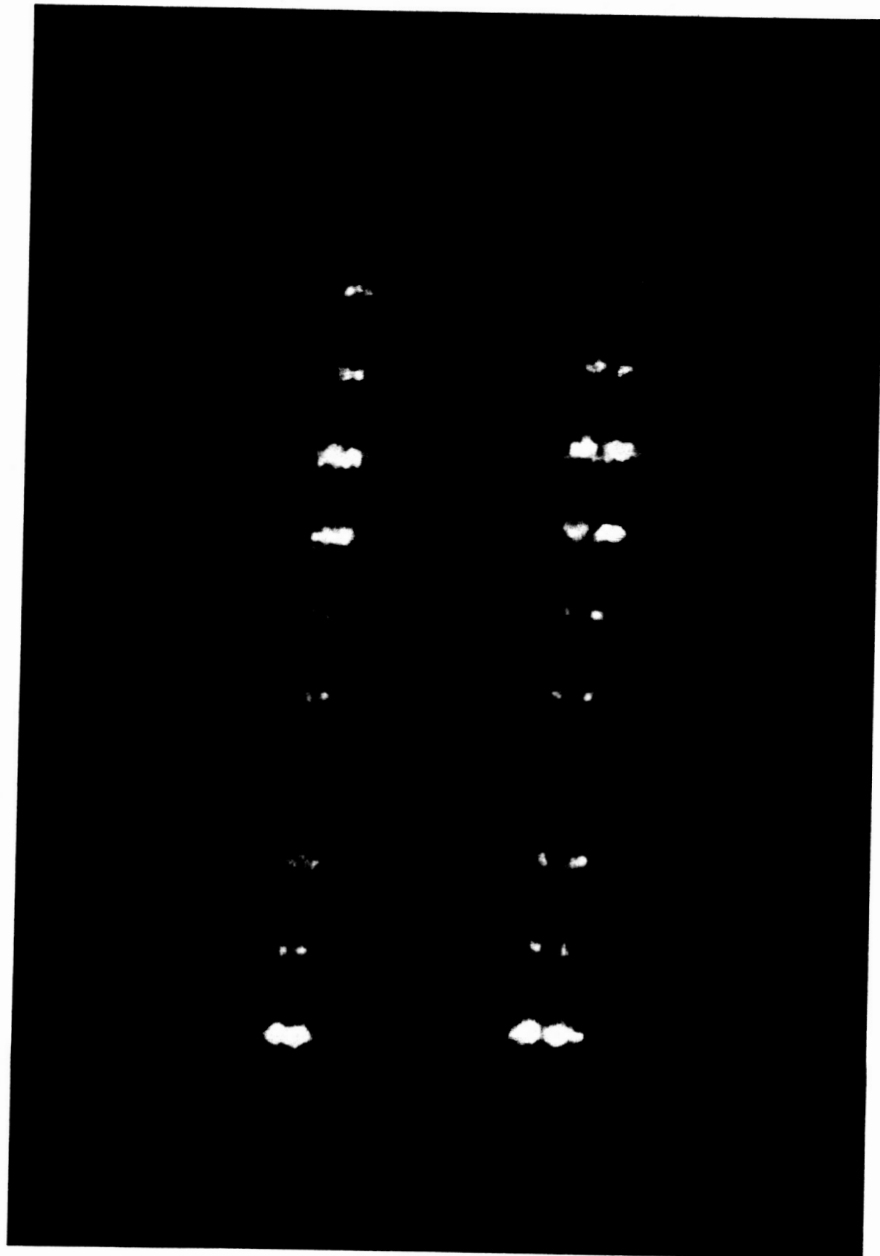


Figure 12

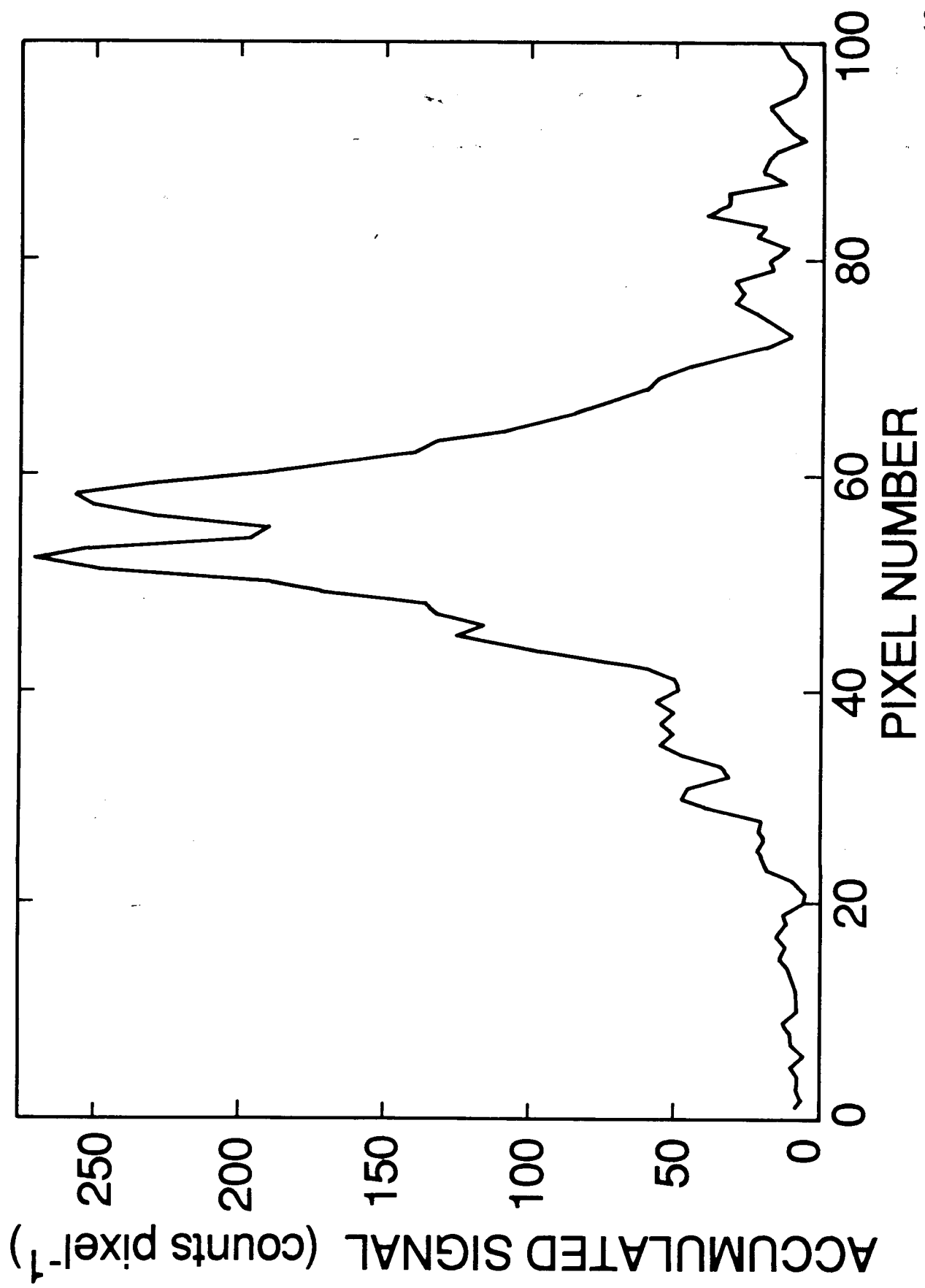


Figure 13 a

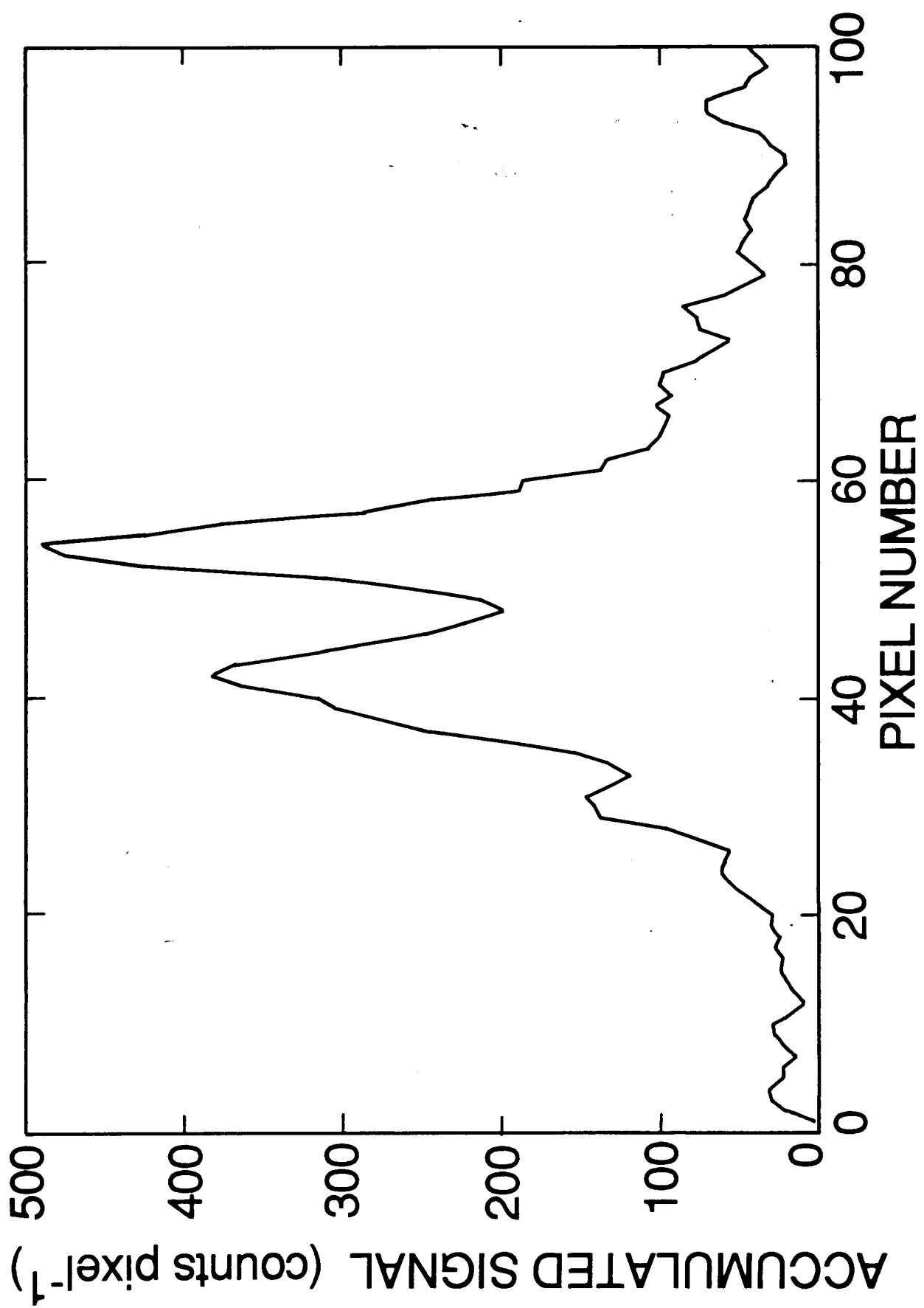


Figure 13 b

A HIGH-RESOLUTION EXTREME ULTRAVIOLET SPECTROHELIOMETER

J.G. Timothy
Center for Space Science and Astrophysics
Stanford University, ERL 314
Stanford, CA 94305 U.S.A.

M.C.E. Huber *
Institut für Astronomie
ETH-Zentrum, CH-8092
Zürich, Switzerland

and

G. Tondello
Istituto di Electronica
Universita di Padova
6/A via Gradenigo, I-35100
Padova, Italy

The extreme ultraviolet (EUV) spectral region at wavelengths below $\sim 1200 \text{ \AA}$ is of critical importance for the diagnostics of conditions in high-temperature plasmas since this region contains emission lines and continua characteristic of temperatures in the range from about 10^4 K to greater than 10^6 K .

Because of the lack of window materials and of high-reflectivity optical surfaces at these wavelengths, practical systems for imaging and spectroscopy must employ open-structure detector systems and a minimum number of reflecting surfaces. The recent development of high-resolution imaging detector systems which can operate with high efficiency at EUV wavelengths¹ has stimulated the design of high-efficiency optical systems which can provide a stigmatic spectroscopic capability at these wavelengths². These imaging spectrometer systems can provide the simultaneous spectral, spatial and temporal resolutions required for many scientific observations that have not been previously possible. We have fabricated and tested toroidal gratings for use in imaging spectrographs at EUV wavelengths by means of a unique technique developed at the Marseille Observatory. This technique uses an elastically deformable grating, which is replicated from a spherical master ruling^{3,4,5}. We are currently planning the fabrication of aspheric gratings to correct higher-order aberrations using the same technique.

The schematic of a high-resolution EUV spectroheliometer using a toroidal grating spectrometer behind a Gregorian telescope is shown in Figure 1. The key characteristics of this spectroheliometer are listed in Table 1 and the expected output count rates for the strongest emission lines in a 100\AA bandpass centered near 600\AA are listed in Table 2.

Although the spectroheliometer has been configured to fit in a Black Brant sounding rocket, it could easily be accommodated in the e-HRSO Combined Instrument Package (CIP) to provide simultaneous high spatial resolution data from the chromosphere, transition region and corona.

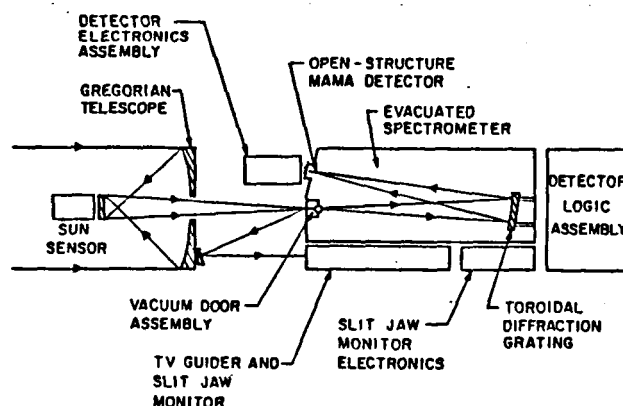


Figure 1. Schematic of a high-resolution EUV Spectroheliometer.

* Currently on leave at the Space Science Department of the European Space Agency (ESA), ESTEC Postbus 299, NL-2200 Noordwijk, The Netherlands.

TABLE 1. Characteristics of the High-Resolution EUV Spectroheliometer

Telescope:

Type: f/15 Gregorian with f/2.5 primary mirror
Diameter of primary mirror: 380 mm
Focal length: 5700 mm
Plate scale in the focal plane: 28 μm per arc sec.

Spectrometer:

Type: Rowland mounting with toroidal or aspheric grating
Entrance slit: 14 μm by 6.2 mm
Instantaneous field-of-view: 0.5 arc sec. by 3.7 arc min.
Stigmatic wavelength range: $\sim 120 \text{ \AA}$
Spectral resolution (2 detector pixels): 78 mÅ

Detector:

Type: Open-structure Multi-Anode Microchannel Array (MAMA)
Format: 440 x 3480 pixels (fine-fine configuration)
Total number of amplifiers: 160
Pixel dimensions: 14 x 14 μm^2
Position sensitivity: $< 1 \mu\text{m}$ (signal-to-noise limited)
Photocathode material: CsI or KBr

TABLE 2. Expected Count Rates from the EUV Spectroheliometer.

ION	λ (Å)	T (K)	INTENSITY ($\text{erg cm}^{-2} \text{ s}^{-1} \text{ sr}^{-1}$) ^a			OUTPUT COUNT RATE ^b ($\text{pixel}^{-1} \text{ s}^{-1}$)		
			Quiet Region	Coronal Hole	Active Region	Quiet Region	Coronal Hole	Active Region
He I	584.3	3.2×10^4	550	250	7200	189	87	2478
He I	537.3	3.2×10^4	71	34	830	22	11	271
O III	599.6	1.3×10^5	31	28	74	11	10	26
O V	629.7	2.5×10^5	330	290	1300	130	109	484
Ca X	574.0	2.5×10^5	7.8	3.1	46	3	1	15
Mg X	625.2	1.8×10^6	51	2.6	470	19	1	177
Si XII	521.1	2.2×10^6	25	-	720	8	-	224

a.. From J.E. Vernazza and E.M. Reeves, *Astrophys. J. Suppl.* 37, 485. (1987).

b. Assumes effective telescope collection area of 50 cm^2 ; grating efficiency 0.10; detector efficiency 0.4 counts photon⁻¹ and a pixel size of $0.5 \times 0.5 \text{ arc.sec}^2$.

Acknowledgements

We are happy to acknowledge Mr. B. Bach of Hyperfine Inc.⁶ for his efforts with the ruling of the master grating and with the fabrication of the toroidal replica gratings. This work was supported in part by the Ministero Pubblica Istruzione, in part by the Schweizerischer Nationalfonds and in part by NASA Grants NAGW-540, NAGW-551 and NASA Contract NASW-4093.

References

1. Timothy, J.G., "Multi-anode Microchannel Array Detector Systems: Performance Characteristics, "Optical Engineering 24, p. 1066, 1985.
2. Huber, M.C.E., Jannitti, E., Lemaître, G., and Tondello, G., "Toroidal Grating on an Elastic Substrate, "Applied Optics 20, p. 2139, 1981.
3. Huber, M.C.E., Jannitti, E., Lemaître, G., and Tondello, G., "Toroidal Grating Obtained on an Elastic Substrate, "Applied Optics 20, p. 2139, 1981.
4. Huber, M.C.E., Timothy, J.G., Morgan, J.S., Lemaître, G., Tondello, G., Puiatti, M.E., and Scarin, P., "An Imaging Extreme Ultraviolet Spectrometer for Astrophysical Investigations in Space, "SPIE Instrumentation in Astronomy VI 627, p. 363, 1986.
5. Huber, M.C.E., Timothy, J.G., Morgan, J.S., Lemaître, G., Tondello, G., Jannitti, E., and Scarin, P., "The Initial Evaluation of An Imaging Extreme Ultraviolet Spectrometer Employing a Single Toroidal Diffraction Grating", to be submitted to Applied Optics, 1987.
6. Hyperfine Inc., 4946 North 63rd Street, Boulder, CO 80301.